



Rational design of the linkers in targeting chimeras

Cite this: *Chem. Sci.*, 2025, 16, 17595Yiping Duan,^{id} abc^d Michelle Y. Cai,^a Jinyi Xu^{id} *^d and Quanyin Hu^{id} *^{abc}Received 1st July 2025
Accepted 15th September 2025

DOI: 10.1039/d5sc04859a

rsc.li/chemical-science

Targeting chimeras (TACs), such as PROTACs, LYTACs, AUTACs, and ATTECs, have emerged as promising strategies for selectively degrading proteins, including undruggable targets. These approaches leverage bifunctional molecules or molecular glues to selectively degrade specific proteins, offering new therapeutic potential for the diseases that traditional small molecules cannot effectively address. The linker of the TACs serving as a bridge, connecting the target protein ligand and effector protein ligand, plays a critical role in determining the molecule's spatial conformation and overall activity. Recent advances in linker design strategies, such as photo-switchable, cleavable, and flexible linkers, have enhanced the efficacy, selectivity, and spatiotemporal control of TACs. Despite these advances, challenges remain in optimizing linker properties to balance stability, bioavailability, and pharmacokinetics. In this review, we discuss recent advancements in TACs development and summarize the strategies of linkers' design, including traditional/non-traditional, and functionalized linkers of various TACs. Finally, we highlight current challenges in linker design and explore future opportunities and strategies, hoping to provide inspiration for the development of TACs in drug discovery.

1. Introduction

Targeted protein degradation (TPD) technology has evolved over two decades from a proof-of-concept into a compelling direction in modern drug discovery.¹ Among the various TPD approaches, chimeric molecule-based degradation strategies have attracted considerable attention. Particularly, proteolysis-targeting chimeras (PROTACs) have achieved significant progress, with over 20 candidates currently in clinical trials.² Building on this foundation, researchers have expanded PROTACs' design strategies to develop a broader range of TACs, including lysosome-targeting chimeras (LYTACs), autophagy-targeting chimeras (AUTACs), autophagosome-tethering compounds (ATTECs), and molecular glue degraders.³ These innovative approaches extend degradation pathways beyond the traditional ubiquitin-proteasome system (UPS) to lysosomal and autophagy-mediated mechanisms (Fig. 1), significantly broadening the range of druggable targets, including membrane proteins and non-enzymatic proteins.⁴ Compared with small-molecule inhibitors, TACs-based therapeutics offer distinct advantages, such as enabling the degradation of previously "undruggable" targets and overcoming resistance

arising from target mutations. These unique features make TACs degraders a highly promising strategy for treating major illnesses, including cancer, neurodegenerative disorders,⁵ and autoimmune conditions.⁶

A typical TACs molecule consists of three main components: a ligand for the target protein (Warhead), a ligand for the effector protein, and a linker (Fig. 1).⁷ Beyond serving as a bridge, the linker plays a critical role in determining the spatial arrangement of the TACs, stabilizing the ternary complex, and determining degradation efficiency. Linker properties, including length, flexibility, hydrophobicity/hydrophilicity, and metabolic stability, are critical determinants of the druggable and suitable pharmacokinetic properties of TACs.⁸ For instance, an overly short linker may impair effective binding, while an excessively long linker can reduce degradation efficiency or cell permeability.¹ Due to its pivotal role in specificity, stability, and therapeutic efficacy, linker design strategy remains a crucial area of improvement in the development of TACs. Suboptimal linkers can weaken binding affinity, destabilize the ternary complex, or lead to off-target effects. Therefore, optimizing linker design requires balancing several factors, such as length, flexibility, hydrophobicity/hydrophilicity of the chemical structure, and biological stability to maximize TACs' performance.

In recent years, significant efforts have been devoted to optimizing TACs linkers, exploring a variety of novel design strategies. In addition to conventional aliphatic and aromatic linkers, researchers have also developed functionalized linkers,⁹ such as click chemistry-based, photo-switchable, cleavable, and other non-traditional linkers, including self-assembling linkers.¹⁰ Moreover, advanced design techniques, including

^aPharmaceutical Sciences Division, School of Pharmacy, University of Wisconsin–Madison, Madison, WI 53705, USA. E-mail: qhu66@wisc.edu

^bCarbone Cancer Center, School of Medicine and Public Health, University of Wisconsin–Madison, Madison, WI 53705, USA

^cWisconsin Center for NanoBioSystems, School of Pharmacy, University of Wisconsin–Madison, Madison, WI 53705, USA

^dDepartment of Medicinal Chemistry, School of Pharmacy, China Pharmaceutical University, Nanjing, Jiangsu 211198, P. R. China. E-mail: jinyixu@china.com





Fig. 1 Degradation mechanism of PROTACs, LYTAC, ATTEC, and AUTAC.

computer-aided drug designs (CADDs), structure-based approaches, and AI-driven methods, have been increasingly applied to the design of linkers in TACs.¹¹ These approaches have been integrated into TACs' development, enhancing both efficacy and versatility.

In this review, we classify linkers based on their chemical and biological characteristics, summarize representative case studies on linker optimization, and discuss emerging trends, strategies, and challenges in this field. Providing a comprehensive overview of linker chemistries used in various TAC designs, emphasizing their roles in druggability, delivery strategies, recent innovations, and therapeutic applications across disease areas. Through selected case studies, we systematically assess how different linker types affect TACs' performance. We hope this review will serve as a valuable reference, clarifying current challenges, highlighting future opportunities, and offering insights into the development of TACs for drug discovery.

2. Linker types in TACs

The linker in TACs' design plays a pivotal role in influencing efficacy, selectivity, solubility, metabolic stability, and cellular uptake. Recently, various types of linkers have been developed and can be broadly categorized into four classes: traditional linkers, functional linkers, non-traditional linkers, and specific TAC linkers.

As shown in Fig. 2, traditional linkers encompass both flexible and relatively rigid types. Flexible linkers mainly include alkyl-based, polyethylene glycol (PEG)-based, and amide-based structures, while rigid linkers consist of cycloalkane-based, spiro-based, and aryl-based components. These linkers affect molecular properties such as molecular weight (MW), pK_a , $\log S$, $\log D$, and $\log P$, thereby impacting TACs' overall druggability.

Functional linkers include cleavable, photocaged, photo-switchable, and click-based linkers (Fig. 2, top right). Unlike traditional linkers, functional linkers can facilitate cellular uptake and permeability, control TACs activation, and reduce off-target binding and toxicity. In addition, non-traditional linkers such as gold nanoparticle-based linkers, split-and-mix systems, and self-assembly-based linkers have also been investigated (Fig. 2, bottom left). These linkers often improve permeability and enable tissue- or organ-specific targeting. Finally, several specific TAC linkers have been reported, including aptamer-based linkers, short single-stranded DNA linkers, and multivalent aptamer constructs (Fig. 2, bottom right). Notably, the linkers used in ATTECs and AUTACs are primarily adapted from traditional linker frameworks.

2.1 Traditional linker

2.1.1 Traditional aliphatic and aromatic linkers. In recent years, a wide array of PROTACs has been reported, with researchers designing structurally diverse linkers tailored to the unique physicochemical and biological requirements of specific targets (*e.g.*, BCL-X_L,¹² AR,¹³ Tau,¹⁴ BRD2/3/4,¹⁵ HPK1,^{16,17} ALK¹⁸) and a broadened range of E3 ligases (*e.g.*, CRBN,¹⁹ VHL,²⁰ MDM2,^{21,22}) (Fig. 3). The primary goal of these designs is to enhance degradation selectivity and improve the overall efficacy of TAC-based therapeutics. The most commonly used linkers include PEG-based,^{23–26} alkyl-based,^{27–31} cycloalkane-based,^{32–40} spiro-based,^{41–45} and aryl-based linkers.⁴⁶ These linkers are typically conjugated to the ligands through functional groups such as amines, amides, single or multiple C–C bonds, among others. Traditional linkers often feature a combination of hydrophobic segments (*e.g.*, linear or cyclic alkanes) and hydrophilic components (*e.g.*, PEGs, piperidines, piperazines,





Fig. 2 Different types of TAC linkers.

and amides), aiming to balance key drug-like properties such as pK_a , $\log S$, $\log D$, $\log P$, and overall druggability. Moreover, aryl-based linkers, including phenyl derivatives and triazoles,⁴⁷

could offer notable advantages such as increased chemical stability, enhanced rigidity, and improved cell permeability. Overall, the successful design of potent PROTACs heavily relies

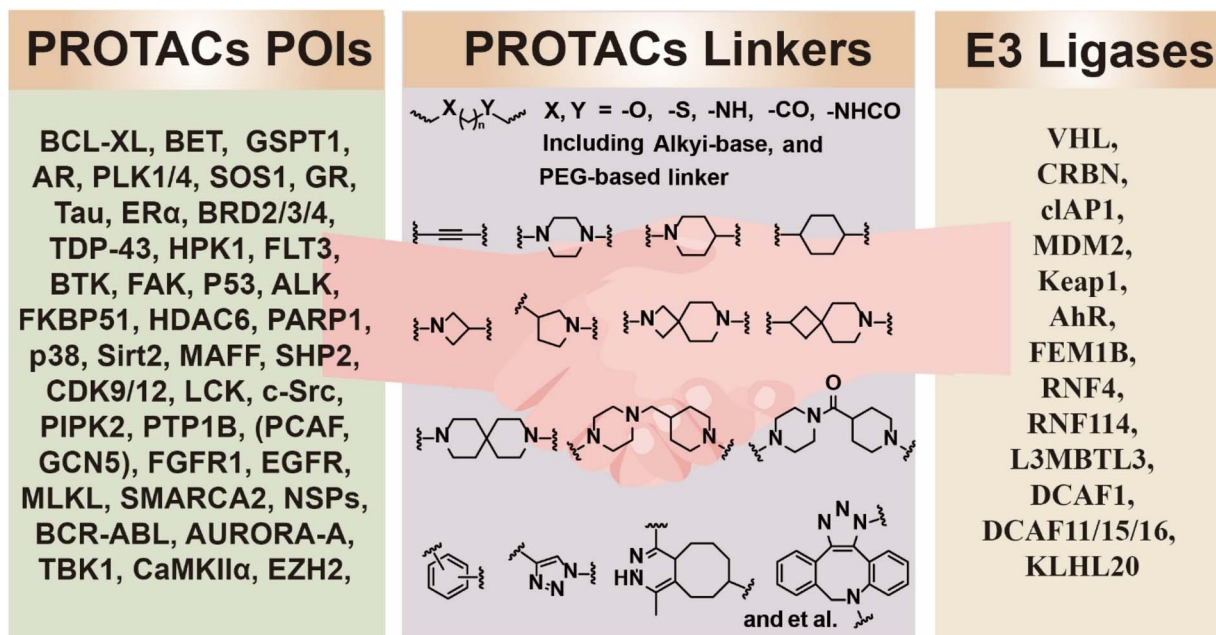


Fig. 3 The various PROTACs with traditional linkers for targeting different proteins and E3 ligases.



on optimizing the linker's length, polarity, and attachment chemistry, which collectively dictate the degrader's efficacy and selectivity.⁴⁸

Although numerous types of traditional TAC linkers have been designed, their ability to balance druggability and degradation efficiency remains limited. To enable the rational design of linkers and PROTACs, Weng *et al.* collected and analyzed structural information on PROTACs from the literature and databases, and subsequently developed the freely accessible PROTAC database (PROTAC-DB: <https://cadd.zju.edu.cn/protacdb/>).⁴⁹ Based on PROTAC-DB, they later upgraded the database, releasing PROTAC-DB 2.0 (ref. 50) and PROTAC-DB 3.0.⁵¹

2.1.2 Trivalent Y-type linker PROTAC. Conventional PROTACs are bivalent molecules designed to simultaneously engage an E3 ligase and a POI through two distinct ligands. To enhance degradation efficiency, researchers have adopted a convergent strategy by incorporating trifunctional Y-type core linkers that connect independent inhibitors and E3 ligands.

Imaide *et al.* hypothesized that increasing binding valency within a PROTAC could improve degradation efficiency. They designed trivalent PROTACs (compound **1-1**), composed of a bivalent bromodomain (BRD) proteins inhibitor and an E3 ligase ligand linked through a Y-type linker (Fig. 4a).⁵² Compared to conventional bivalent PROTACs, compound **1-1** exhibited more potent and sustained degradation activity, translating to enhanced anticancer efficacy. Mechanistically, **1-1** simultaneously engages both BRDs intramolecularly with high avidity and forms a 1:1:1 ternary complex with von hippel-

lindau (VHL). This configuration shows positive cooperativity, increased cellular stability, and prolonged residence time.

Zheng *et al.* employed a different strategy to construct Y-type linker PROTACs, synthesizing dual-targeting molecules capable of degrading two distinct proteins simultaneously.⁵³ By combining gefitinib, olaparib, and a cereblon (CRBN) ligand, while using trifunctional natural amino acids as the core linker, they developed dual PROTACs (compound **1-2**, Fig. 4b). These compounds successfully induced the simultaneous degradation of both the epidermal growth factor receptor (EGFR) and poly (ADP-ribose) polymerase (PARP) in cancer cells.

Precise tissue-selective degradation is crucial for minimizing off-target toxicity in PROTAC development. Folate receptor α (FOLR1) has been extensively validated as a target for cancer-specific drug delivery, characterized by its overexpression in various malignancies and limited or absent expression in normal tissues.⁵⁴ Liu *et al.* introduced a cancer cell-selective delivery approach by conjugating a folate group to a VHL ligand, yielding a trivalent PROTAC (compound **1-3**, Fig. 4c).⁵⁵ This molecule selectively degraded BRD family proteins in folate receptor-expressing cancer cells, sparing normal tissues.

In addition, trivalent PROTACs have demonstrated dual-target degradation capabilities. Recruiting two different E3 ligases within a single molecule offers a promising alternative strategy. Bond *et al.* designed hetero-trivalent PROTACs (compounds **1-4**, Fig. 4d), incorporating ligands for CRBN, VHL, and bromodomain and extraterminal (BET) proteins *via* a branched trifunctional linker.⁵⁶ Experiments in wild-type, single-ligase knockout, and double-ligase knockout cell lines



Fig. 4 (a–d) Representative examples of trivalent Y-type linker PROTACs.



revealed that degradation induced by 1-4 was mediated additively by both CRBN and VHL, validating the dual-ligase recruitment approach.

2.2 Functionalization linker

2.2.1 Click chemistry-based linkers. Click chemistry refers to a class of highly efficient, selective, and bioorthogonal reactions first introduced by K. Barry Sharpless in 2001.⁵⁷ These reactions have transformed chemical biology and medicinal chemistry, enabling rapid and reliable molecular assembly for applications in drug discovery, biomolecule labeling, and targeted therapeutics.⁵⁸ Owing to their high efficiency and biocompatibility, several *in vitro* and *in vivo* click chemistry-based PROTACs have recently been developed.

Lebraud *et al.* reported the first in-cell click-formed proteolysis targeting chimeras (CLIPTACs), in which two fragments are ligated *via* bioorthogonal click reactions (Fig. 5a).⁵⁹ Specifically, they designed a tetrazine (TZ)-labeled thalidomide and a *trans*-cyclooctene (TCO)-tagged ligand targeting BRD4 or extracellular regulated protein kinases 1/2 (ERK1/2). The

resulting CLIPTACs (2-1a and 2-1b) successfully degraded their respective targets intracellularly. This modular approach offers several advantages, such as overcoming the high molecular weight limitations of conventional PROTACs and enhancing solubility and cell permeability. However, this study was limited to the *in vitro* experiments and did not evaluate *in vivo* efficacy.

More recently, Teng *et al.* introduced the ClickRNA-PROTAC system (Figure 5b),⁶⁰ which utilizes mRNA-directed expression of SNAP-tag (2-2a) and HaloTag (2-2b) fusion proteins. These tags are covalently linked *via* bioorthogonal click chemistry to recruit and degrade target proteins. ClickRNA-PROTAC enabled efficient degradation of various POIs, including BRD4, Kirsten rat sarcoma viral (KRAS), and nuclear factor kappa-B (NFκB), by simply exchanging the warhead ligands. Notably, a tumor-specific mRNA-responsive translation strategy allowed selective degradation in cancer cells. *In vivo*, the system demonstrated potent antitumor activity in a xenograft model of adrenocortical carcinoma, highlighting its therapeutic potential.

Xie *et al.* developed Nano-Click-formed PROTACs (Nano-CLIPTACs) for both *in vitro* and *in vivo* applications (Fig. 5c).⁶¹

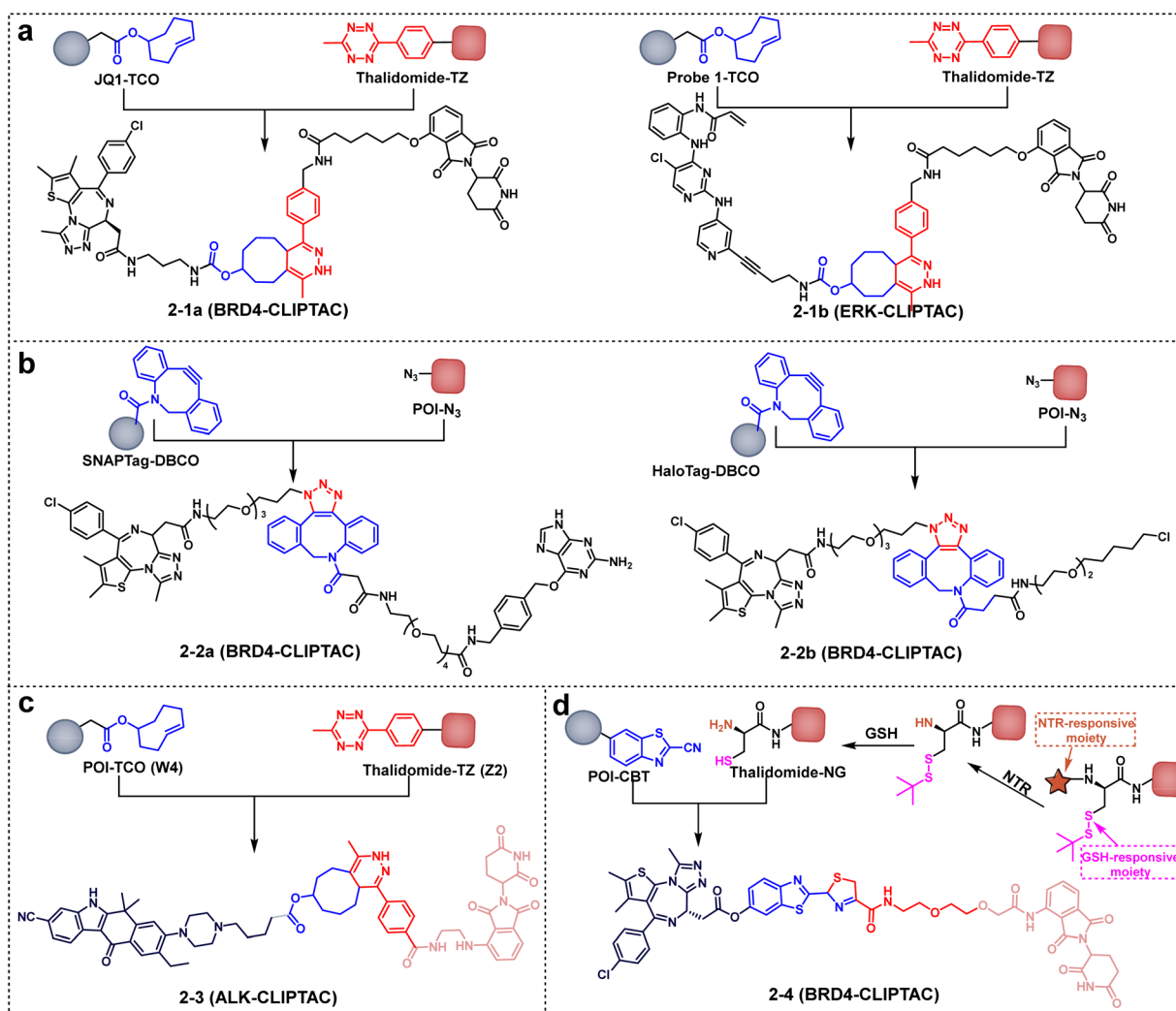


Fig. 5 (a–d) Representative of the self-assembly of CLIPTACs.



Unlike conventional PROTACs, Nano-CLIPTACs divide the PROTAC molecule into two smaller fragments that can self-assemble into a functional degrader through a bioorthogonal click reaction between the TCO and TZ group. To achieve tumor-targeted delivery and *in situ* self-assembly, the authors encapsulated the individual fragments (**W4** and **Z2**) into cyclic RGDfC-peptide-modified liposomes, resulting in the formation of Nano-CLIPTAC 2-3. The targeting of echinoderm microtubule-associated protein-like 4/anaplastic lymphoma kinase (EML4-ALK) as the POI and recruiting CRBN as the E3 ligase demonstrated effective degradation. This innovative approach of linker design not only enhances tumor specificity but also addresses limitations of traditional PROTACs, such as off-target effects and the “hook effect.”

Do *et al.* introduced a novel class of enzyme-derived clicking PROTACs (ENCTACs), which allow for orthogonal cross-linking of two distinct small-molecule ligands targeting BRD4 and an

E3 ligase exclusively in hypoxic tumor environments (Fig. 5d).⁶² In this system, nitroreductase (NTR)-responsive moiety undergoes self-immolation, releasing an amine group. Concurrently, glutathione (GSH)-sensitive group is cleaved in the tumor microenvironment to liberate a thiol group, generating the E3 ligase ligand (Thalidomide-NG). Finally, 2-cyano-benzothiazole (CBT) substituted POI ligand (POI-CBT) undergoes self-assembly click reaction *in vitro* or *vivo* to generate the ENCTACs 2-4. This dual-responsive system provides spatial and environmental control over PROTAC assembly, offering a promising strategy for precise, tumor-selective protein degradation.

2.2.2 Photo-switchable linkers. In recent years, increasing attention has been directed towards the development of functional linkers in PROTACs. Beyond conventional click-based linkers, photo-switchable groups have emerged as powerful tools for spatiotemporal control of protein degradation.⁶³ One



Fig. 6 Representative of the PHOTACs.



notable strategy involves incorporating azobenzene (Azo) photo-switches into the linker region, yielding light-inducible PROTACs, commonly referred to as PHOTACs. These can be toggled between active and inactive forms using specific wavelengths (Fig. 6).

Pfaff *et al.* introduced PHOTAC 3-1, which uses an Azo linker.⁶⁴ The *cis*-isomer of 3-1, due to its shorter linker length in the three-dimensional structure, is inactive and prevents ternary complex formation. In contrast, the *trans*-isomer enables proper engagement of both target and E3 ligase, triggering degradation. Additionally, the inclusion of an ortho-F4-substituted Azo moiety ensures a stable photo-stationary state, eliminating the need for continuous irradiation.

Following this, Jin *et al.* reported PHOTAC 3-2,⁶⁵ which demonstrated reversible protein degradation activity regulated by light. By integrating a lenalidomide-Azo-dasatinib tri-functional system, PHOTAC 3-2 enabled light-controlled degradation of ABL and BCR-ABL proteins in intact cells through *trans-cis* isomerization.

Reynders *et al.* further advanced the design PHOTAC 3-3,⁶⁶ in which the thalidomide phenyl ring of compound 3-3 was directly integrated into the Azo linker. This construct targeted BRD2/3/4 and exhibited minimal activity in the dark, but could be reversibly activated by specific wavelengths, offering precise optical control over protein levels. This approach represents a promising strategy to reduce systemic toxicity and improve therapeutic precision.

Ko *et al.* described a Ca²⁺/calmodulin-dependent protein kinase II alpha (CaMKII α) targeting PHOTAC (3-4) featuring a thalidomide-conjugated Azo linker.⁶⁷ This construct demonstrated reversible, light-regulated degradation of CaMKII α in mouse brain tissue, marking the first successful application of PHOTACs for optical protein control in neural systems.

Zhang *et al.* introduced PHOTACs 3-5a and 3-5b based on a novel arylazopyrazole linker,⁶⁸ which provided enhanced photo-switching efficiency compared to traditional Azo-based linkers. With BRD4 or multi-kinase inhibitors as warheads, and CRBN recruiters (thalidomide or lenalidomide), these PHOTACs reached a 75% *trans*-isomer ratio under 457 nm light and 99% *cis*-isomer under 365 nm. This system exhibited

distinct and improved photochemical properties compared with Azo-linker PHOTACs.

Cheng *et al.* developed PHOTAC 3-6, the first chemical tool to optically control nicotinamide adenine dinucleotide (NAD⁺) metabolism by targeting nicotinamide phosphoribosyltransferase (NAMPT) using an arylazopyrazole linker.⁶⁹ This construct allowed reversible regulation of NAMPT activity and NAD⁺ levels, with reduced toxicity compared to conventional PROTACs. Notably, under 620 nm light, PHOTAC 3-6 enabled *in vivo* antitumor activity modulation, marking the first *in vivo* therapeutic application of a PHOTAC.

Most recently, Zhang *et al.* reported the first photo-switchable molecular glues (MGs) for light-controlled protein dimerization and degradation.⁷⁰ These MGs consist of a covalent protein ligand, an eDHFR-binding moiety, and a photo-switchable core. Uniquely, they replaced the commonly used Azo switch with a diazocine linker, leading to MG 3-7. This system responded to 405 nm and 530 nm light for *cis-trans* interconversion, enabling repeated cycles of protein stabilization or degradation with high spatiotemporal precision.

2.2.3 Photo-caged linkers. In addition to photo-switchable linkers, researchers have also developed photo-caged PROTACs (pc-PROTACs), which incorporate light-sensitive groups that undergo irreversible photo-cleavage upon exposure to specific wavelengths.⁷¹ This light-triggered removal of the protective group activates the PROTAC, enabling targeted protein degradation. Such designs offer spatiotemporal control and help mitigate off-target toxicity (Fig. 7). Xue *et al.* reported a representative pc-PROTAC,⁷² in which a photo-removable caging group was introduced into a BRD4-targeting degrader to generate compound pc-PROTAC 4-1a. Upon light irradiation, the caging group was cleaved, releasing the active degrader 4-1b. This compound demonstrated efficient BRD4 degradation in live cells exclusively after light activation. Moreover, pc-PROTAC 4-1a also effectively degraded BRD4 in zebrafish models and induced the expected phenotypic responses.

2.2.4 Cleavable linkers. Recently, our group introduced a novel *N*-acyl-*N*-alkyl sulfonamide (NASA) linker into PROTACs, enabling covalent labeling of the POI.⁷³ Chen *et al.* from our group developed a strategy to engineer platelets capable of



Fig. 7 Representative of the pc-PROTACs.





Fig. 8 Representative of the cleavable linkers in PROTAC designs.

degrading both intracellular and extracellular POIs *in vivo*. This approach relies on covalently linking a POI ligand to heat shock protein 90 (HSP90) within platelets. As shown in Fig. 8, this platelet-based TPD method involves functionalizing heat shock protein 90 (HSP90) with the POI ligand, generating degrader platelets (DePLTs). These DePLTs selectively accumulate in hemorrhagic areas and exploit HSP90's protein processing role to facilitate POI degradation. In this system, cleavable NASA linker-based PROTACs 5-1a and 5-1b are designed to covalently modify HSP90 in platelets. Through the endogenous transport pathway of HSP90, these modified PROTACs generate DePLTs. Upon activation, DePLTs enable efficient degradation of POIs either *via* the ubiquitin proteasome pathway for intracellular targets or through lysosomal mechanisms for extracellular ones.

2.3 Non-traditional linker

2.3.1 Split-and-mix linkers. Compared to traditional PROTAC linkers, split-and-mix PROTACs (SM-PROTACs) represent a non-traditional strategy that separates the POI-binding moiety and the E3 ligase ligand (split), allowing for their self-assembly (mix) into functional degraders both *in vitro* and *in vivo*, rather than relying on direct conjugation into a single molecule. SM-PROTACs act as a special nanoplatform for facile screening and self-optimized biomolecular regulation.⁷⁴ Specifically, this system consists of independently modified POI and E3 ligase ligands, each equipped with self-assembling segments (Fig. 9). Due to the nature of this system, SM-PROTACs can generate multivalent PROTACs with tunable ratios of E3 recruiters and POI binders.

In 2023, Yang *et al.* introduced a SM-PROTAC platform based on diphenylglycine peptides ($\delta\delta\text{RR}$) capable of self-assembly.⁷⁵ By modifying estrogen receptor alpha ($\text{ER}\alpha$), cyclin-dependent kinase 4/6 (CDK4/6), androgen receptor (AR), mitogen-activated protein kinase 1/2 (MEK1/2), BRD2/4, and BCR-ABL ligands with $\delta\delta\text{RR}$, and similarly modifying CRBN and VHL ligands generated split moieties, a library of SM-PROTACs was constructed through modular mixing (Fig. 9a). These SM-PROTACs demonstrated effective POI degradation *in vitro*,

validating both the efficacy and general applicability of the platform for proximity-induced degradation.

In the same year, Song *et al.* developed another split-and-mix nanoplatform based on liposome self-assembly for multifunctional applications.⁷⁶ Using $\text{ER}\alpha$ as the model POI, they incorporated folic acid (FA) to improve tumor targeting. FA, tamoxifen (Tam), and a VHL ligand were individually modified with DSPE-PEG2000 and then combined using the split-and-mix strategy to form a trivalent SM-PROTAC (Fig. 9b). The resulting construct exhibited efficient and selective uptake in folate receptor-positive (FR^+) cells and successfully degraded $\text{ER}\alpha$ at significantly reduced concentrations.

In a follow-up study, Song *et al.* further expanded the SM-PROTAC platform to target MEK and ALK.⁷⁷ DSPE-PEG2000 was used to modify mirdametinib (MEK inhibitor), ceritinib (ALK inhibitor), and a VHL ligand, creating the split moieties. These moieties were then mixed to generate two SM-PROTACs (Fig. 9c), which effectively degraded MEK1/2 in A375 cells and ALK in NCI-H2228 cells, respectively, showing marked tumor inhibition. Notably, these SM-PROTACs exhibited excellent biocompatibility, *in vivo* efficacy, and safety.

2.3.2 Self-assembly Nano-TACs linkers. Taking advantage of the SM-PROTACs strategy, Zhang *et al.* developed an intracellularly assembled Nano-PROTAC system featuring a center-spoke E3 ligase-POI degradation network to achieve dose-dependent and long-lasting degradation both *in vitro* and *in vivo*.⁷⁸ Specifically, the Nano-PROTAC system comprises two hydrophilic self-assembling peptides functionalized with azido or alkyne groups, each conjugated to either a POI ligand or an E3 ligase ligand (Fig. 10a). In the presence of high glutathione (GSH) levels, these two components undergo click chemistry to form assembly-driving monomers. These monomers then rapidly self-assemble into antiparallel β -sheet nanostructures within the cytoplasm. The Nano-PROTACs exhibited potent degradation activity against two representative targets, EGFR and AR, both *in vitro* and *in vivo*.

Zhang *et al.* further introduced a smart Nano-PROTAC (SPN) system designed to target cyclooxygenase-1/2 (COX-1/2) for photoactivatable metabolic cancer immunotherapy (Fig. 10b).⁷⁹ This SPN_{COX} is built on a semi-conducting polymer backbone,





Fig. 9 (a–c) Representative of the SM-PROTACs.

conjugated to a COX1/2-targeting PROTAC peptide (CPP) via a cathepsin B (CatB)-cleavable linker. In the tumor microenvironment, overexpressed CatB cleaves the linker to release the active CPP, which then recruits COX1/2 via an indomethacin unit and engages the VHL E3 ligase via a VHL-targeting moiety. This results in sustained degradation of COX1/2 through the ubiquitin proteasome system. The study demonstrated that SPN_{COX}, upon photo-activation, effectively inhibits tumor growth, metastasis, and recurrence in mouse models.

In 2024, Sun *et al.* reported a self-assembled nanoparticle-based molecular glue system (nano-mGlu) using a newly identified Bcr-Abl degrading molecular glue (H1-mGlu),⁸⁰ modified with a PEG-based self-assembling segment (Fig. 10c). The nano-H1-mGlu system responds to high intracellular concentrations of GSH or H₂O₂, releasing the active H1-mGlu *in vitro*. Furthermore, nano-H1-mGlu induced specific degradation of endogenous Bcr-Abl in K562 cells and demonstrated significant antitumor efficacy in a K562 xenograft mouse model, leading to pronounced tumor regression.

2.3.3 Gold nanoparticle-based multi-headed linkers. In addition to self-assembling PROTACs, Wang *et al.* developed a novel gold nanoparticle (GNP)-based multi-headed PROTAC platform targeting ALK for degradation.⁸¹ Ceritinib and pomalidomide were employed as the ALK-targeting ligand and the E3 ligase ligand, respectively. PEG chains were functionalized with either ceritinib or pomalidomide at one end and a sulfhydryl group at the other. These sulfhydryl-modified moieties were then anchored onto the GNP surface, which served as a unique multivalent linker (Fig. 11). The resulting GNP-PROTAC efficiently reduced ALK fusion protein levels in a dose- and time-dependent manner, and specifically suppressed the proliferation of NCI-H2228 cells. Compared with traditional PROTACs, this GNP-based PROTAC promotes the formation of coacervates involving POIs, multi-headed PROTACs, and E3 ubiquitin ligases, where the POI and E3 ligase interact through multidirectional ligands and a flexible linker, thereby bypassing the need for complex structural optimization.





Fig. 10 (a–c) Representative of the self-assembly nano-TACs Linkers. Partial (a) was adapted from ref. 78. Reproduced with permission. Copyright 2023, Wiley.



Fig. 11 Representative of the GNP-based PROTACs linker.

2.4 Linker design in specific TACs modalities

The fundamental principle of TACs-based degraders is their dependence on recruiting target proteins to intracellular degradation pathways *via* small molecules or chimeric constructs. For instance, LYTACs mediate ligand-dependent

endocytosis by binding to transmembrane receptors such as cation-independent mannose-6-phosphate receptor (CI-M6PR) or asialoglycoprotein receptor (ASGPR), thereby directing target proteins to lysosomes for degradation.^{82,83} In contrast, AUTACs and ATTECs go through ubiquitination or autophagy-



platelet-derived growth factor (PDGF) and the membrane protein tyrosine kinase 7 (PTK7).

Building on this concept, Sun *et al.* reported bispecific aptamer chimeras (ITGBACs) targeting integrin $\alpha 3 \beta 1$ (ITGA3B1) in 2024 (Fig. 13b).⁸⁸ ITGBACs are composed of two aptamers: one that targets ITGA3B1 and another that binds to the membrane-associated POI, enabling efficient lysosomal degradation of the POI. Experimental results demonstrated that ITGBACs successfully eliminated pathological membrane proteins such as transferrin receptor protein 1 (CD71) and PTK7, leading to pronounced cell cycle arrest, increased apoptosis, and significant inhibition of tumor growth in mouse tumor models.

Subsequently, Duan *et al.*, from the same research group, developed a modular multivalent Apt-LYTAC platform to investigate the effect of aptamer valency on degradation efficiency (Fig. 13c).⁸⁹ The platform utilizes biotin-streptavidin assembly, with streptavidin (SA) conjugated to aptamers at specific molar ratios and biotin-modified polymannose-6-phosphate (bpM6P) polymers targeting CI-M6PRs. The results showed that multivalent Apt-LYTACs significantly enhanced the degradation of surface proteins such as PTK7 and Met compared to their monovalent counterparts, with optimal efficacy observed within a defined aptamer-to-SA stoichiometric range.

2.4.2 AUTACs and ATTECs linkers. AUTACs and ATTECs are emerging small-molecule approaches that harness the autophagy lysosome pathway for selective protein degradation.⁹⁰ AUTACs are bifunctional molecules that consist of a target-binding ligand, a guanine-based degradation tag, and

a linker, collectively marking proteins for selective autophagic degradation. In contrast, ATTECs function as molecular glues that directly link target proteins to light chain 3 (LC3) on autophagosomes, facilitating their degradation *via* autophagy without requiring a distinct degradation tag or even a linker (Fig. 14).⁹¹ Compared to LYTACs, both AUTACs and ATTECs typically utilize conventional linkers. However, due to the glue-like mechanism of ATTECs, the presence of the linker is not strictly necessary for their activity.

Pei *et al.* designed a novel class of AUTACs to target BRD4 by leveraging LC3 as the autophagy mediator.⁹² Among them, compound **6-1**, featuring a PEG linker, demonstrated potent BRD4 degradation and strong anti-proliferative activity in various tumor cell lines.

Takahashi *et al.* reported a second-generation AUTACs strategy utilizing alkylguanine as the degradation tag,⁹³ inspired by autophagic pathogen clearance mechanisms. The represented AUTAC **6-2** effectively degraded FKBP12-binding protein 12 (FKBP12) in HeLa cells.

Dong *et al.* introduced an ATTEC that selectively degraded NAMPT using a novel ispinesib-based LC3 warhead.⁹⁴ Compound **6-3**, combining a NAMPT inhibitor and an LC3 ligand *via* a flexible linker, significantly reduced NAMPT levels and showed strong antitumor activity in cells.

Later, Bao *et al.* from the same research group developed the phosphodiesterase δ (PDE δ)-targeting ATTECs.⁹⁵ The most promising compound **6-4** showed potent PDE δ -binding affinity and induced efficient degradation without altering PDE δ mRNA expression. It outperformed traditional PDE δ inhibitors in KRAS-mutant pancreatic cancer models.

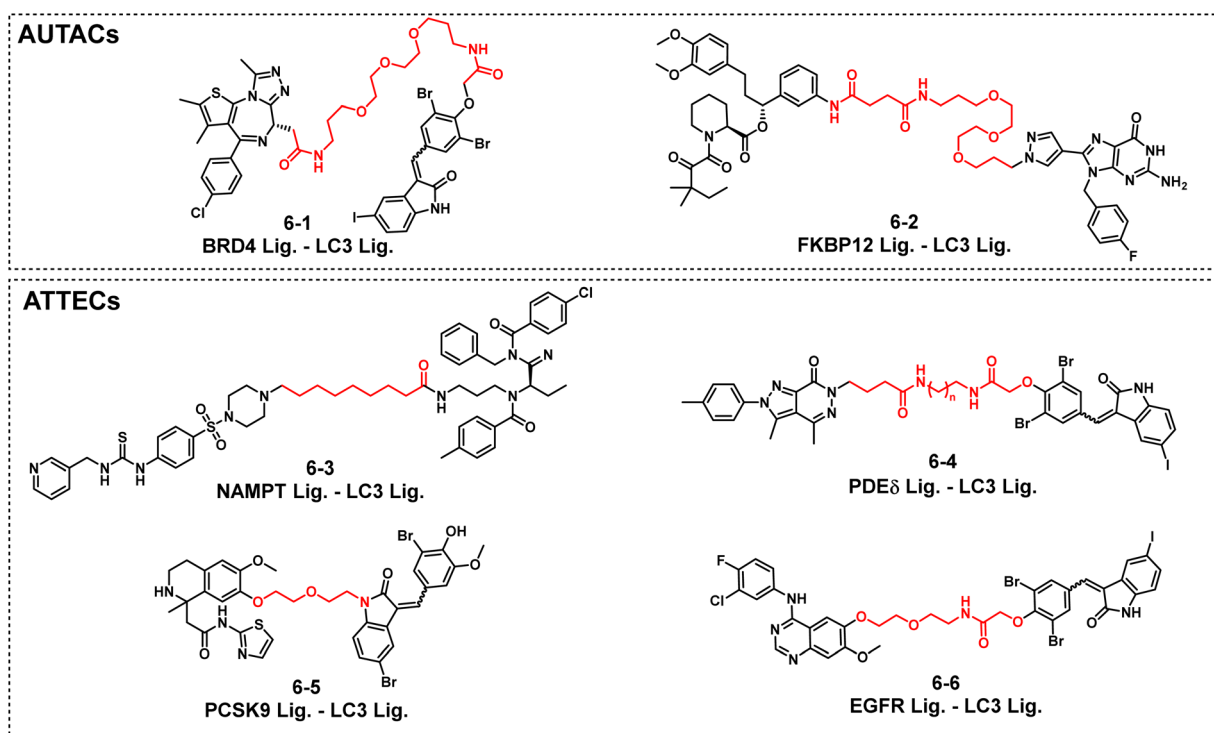


Fig. 14 Representative of AUTACs and ATTECs based on traditional linkers.



Ouyang *et al.* reported a series of proprotein convertase subtilisin/kexin type-9 (PCSK9) directed ATTECs capable of lowering PCSK9 levels *via* autophagy.⁹⁶ Among them, compound 6-5, equipped with a flexible PEG linker, outperformed simvastatin in reducing low-density lipoprotein cholesterol levels and improving atherosclerosis *in vivo*.

Zhu *et al.* developed EGFR-targeting ATTECs,⁹⁷ which tethered EGFR to LC3B using the LC3 ligand GW5074. Their representative molecule 6-6 effectively induced EGFR degradation in HCC827 cells and exhibited promising *in vivo* antitumor efficacy.

3. Challenges and future opportunities

Although the development of TACs is progressing rapidly, the design of optimal linkers that connect the target-binding moiety to the recruiter (*e.g.*, E3 ligase ligands or lysosome-targeting ligands) remains a major challenge.^{7,48} However, linkers significantly influence the physicochemical properties, biological activity, selectivity, and pharmacokinetics of TACs.⁹⁸ Achieving an optimal linker of the TACs that balances stability, bioavailability, pharmacokinetics, and efficacy requires innovative strategies and interdisciplinary collaboration. In addition, considerations such as balancing linker flexibility and rigidity, enhancing metabolic stability, and optimizing pharmacokinetics across different TAC platforms are also crucial. Unlike traditional drug development, the design of linkers for different TACs lacks systematic design principles, making it difficult to predict linker properties. Furthermore, the multi-step synthesis and diversification of linkers may be time-consuming and costly, posing additional barriers to TACs development.

Despite these challenges, there are clear opportunities for optimization of linkers through innovative research. For instance, rational linker design aided by computational modeling, such as molecular dynamics simulations, AI-based predictive models, and ternary complex docking, holds great promise.⁹⁹ In addition, multifunctional linkers (*e.g.*, clickable, photo-switchable, or cleavable) warrant further investigation. Finally, HTS of diverse linker libraries (*e.g.*, through DNA-encoded libraries or fragment-based approaches),¹⁰⁰ combined with machine learning techniques to identify optimal TAC linkers, represents a promising future direction.

4. Conclusion and perspective

TPD technologies, including PROTACs, LYTACs, AUTACs, and ATTECs, have revolutionized drug discovery by enabling the selective degradation of disease-associated proteins, including those previously considered “undruggable” targets.¹⁰¹ Advances in linker design, such as the incorporation of click chemistry, photo-switchable, cleavable, and self-assembling linkers, have broadened the utility of these degraders, enhancing their specificity and therapeutic efficacy.¹⁰² The platforms also introduce novel mechanisms to modulate biological pathways

through controlled protein elimination. Nevertheless, several challenges remain, particularly in optimizing linker design. Achieving an optimal linker that balances flexibility, stability, pharmacokinetics, and efficacy continues to be a major hurdle. The absence of systematic design rules and the complexity of multi-step linker synthesis further impede the rapid development of TAC-based therapies.

Taken together, future efforts should focus on the development of efficient and predictive linker design strategies by integrating computational modeling, machine learning, and HTS. Additionally, continued exploration of multifunctional linkers such as those incorporating clickable or photo-responsive functionalities will enhance the versatility and precision of TAC platforms. With sustained research and innovation, TPD technologies hold great promise for expanding the therapeutic landscape and addressing a wider range of diseases.

Author contributions

All authors contributed to the writing and revision of the manuscript.

Conflicts of interest

The authors declare no competing financial interest.

Data availability

No primary research results, software or code have been included and no new data were generated or analyzed as part of this review.

Acknowledgements

This work was supported by the start-up package from the University of Wisconsin-Madison.

References

- 1 G. Zhong, X. Chang, W. Xie and X. Zhou, *Signal Transduct. Target. Ther.*, 2024, **9**, 308.
- 2 J. Zattoni, P. Vottero, G. Carena, C. Oliveto, G. Pozzati, B. Morabito, E. Gitari, J. Tuszyński and M. Aminpour, *Comput. Meth. Prog. Bio.*, 2025, **264**, 108687.
- 3 Y. Chen, I. Tandon, W. Heelan, Y. Wang, W. Tang and Q. Hu, *Chem. Soc. Rev.*, 2022, **51**, 5330.
- 4 V. Haridas, S. Dutta, A. Munjal and S. Singh, *iScience*, 2024, **27**, 109574.
- 5 X. Wang, W. Shuai, P. Yang, Y. Liu, Y. Zhang and G. Wang, *Ageing Res. Rev.*, 2024, **102**, 102584.
- 6 M. S. Galla, N. Sharma, P. Mishra and N. Shankaraiah, *RSC Med. Chem.*, 2024, **15**, 2585.
- 7 Y. Dong, T. Ma, T. Xu, Z. Feng, Y. Li, L. Song, X. Yao, C. R. Ashby and G.-F. Hao, *Acta Pharm. Sin. B*, 2024, **14**, 4266.



- 8 V. Poongavanam, Y. Atilaw, S. Siegel, A. Giese, L. Lehmann, D. Meibom, M. Erdelyi and J. Kihlberg, *J. Med. Chem.*, 2022, **65**, 13029.
- 9 C. Wang, Y. Zhang, S. Yang and D. Xing, *Arab. J. Chem.*, 2023, **16**, 105015.
- 10 Z. Lin, B. A. Garcia and D. Lv, *Angew. Chem., Int. Ed.*, 2024, **63**, e202316581.
- 11 W. Lv, X. Jia, B. Tang, C. Ma, X. Fang, X. Jin, Z. Niu and X. Han, *Eur. J. Med. Chem.*, 2025, **289**, 117432.
- 12 S. Khan, X. Zhang, D. Lv, Q. Zhang, Y. He, P. Zhang, X. Liu, D. Thummuri, Y. Yuan, J. S. Wiegand, J. Pei, W. Zhang, A. Sharma, C. R. McCurdy, V. M. Kuruvilla, N. Baran, A. A. Ferrando, Y.-m. Kim, A. Rogojina, P. J. Houghton, G. Huang, R. Hromas, M. Konopleva, G. Zheng and D. Zhou, *Nat. Med.*, 2019, **25**, 1938.
- 13 W. Xiang, L. Zhao, X. Han, T. Xu, S. Kregel, M. Wang, B. Miao, C. Qin, M. Wang, D. McEachern, J. Lu, L. Bai, C.-Y. Yang, P. D. Kirchhoff, J. Takyi-Williams, L. Wang, B. Wen, D. Sun, M. Ator, R. McKean, A. M. Chinnaiyan and S. Wang, *J. Med. Chem.*, 2023, **66**, 13280.
- 14 B. Gong, W. Zhang, W. Cong, Y. Gu, W. Ji, T. Yin, H. Zhou, H. Hu, J. Zhuang, Y. Luo, Y. Liu, J. Gao and Y. Yin, *Adv. Healthc. Mater.*, 2024, **13**, e2400149.
- 15 M. Zhao, W. Ma, J. Liang, Y. Xie, T. Wei, M. Zhang, J. Qin, L. Lao, R. Tian, H. Wu, J. Cheng, M. Li, Y. Liu, L. Hong and G. Li, *J. Med. Chem.*, 2024, **67**, 19428.
- 16 M. Wu, Y. Wu, Y. Jin, X. Mao, S. Zeng, H. Yu, J. Zhang, Y. Jin, Y. Wu, T. Xu, Y. Chen, Y. Wang, X. Yao, J. Che, W. Huang and X. Dong, *J. Med. Chem.*, 2024, **67**, 13852.
- 17 Z. Zhang, L. Guo, M. Zhao, H. Pan, Z. Dong, L. Wang, X. Yang, Z. Zhang, M. Wu, Y. Chang, Y. Yang, L. Sun, S. Liu, R. Zhu, H. Zheng, X. Dai, X. Zhang, C. Jiang, Z. Zhu, Y. Zhang and D. Liu, *J. Med. Chem.*, 2024, **67**, 18682.
- 18 S. Xie, Y. Sun, Y. Liu, X. Li, X. Li, W. Zhong, F. Zhan, J. Zhu, H. Yao, D.-H. Yang, Z.-S. Chen, J. Xu and S. Xu, *J. Med. Chem.*, 2021, **64**, 9120.
- 19 P. He, C. Wen, X. Zhang and H. Yin, *J. Med. Chem.*, 2025, **68**, 5551.
- 20 Z. Li, L. S. Harikrishnan, G. Xu, D. Samanta, J. C. Clemente, L. Leng, W. Tu, L. Yang, L. Huang, M. Wang, S. Wang, Q. Deng, E. Behshad, R. Nagilla, P. Orth, C. Rice, C. Strickland, H. P. Mohammad, E. S. Priestley and Z. Sui, *J. Med. Chem.*, 2025, **68**, 1134.
- 21 J. Hines, S. Lartigue, H. Dong, Y. Qian and C. M. Crews, *Cancer Res.*, 2019, **79**, 251.
- 22 S. Jeong, J.-K. Cha, W. Ahmed, J. Kim, M. Kim, K. T. Hong, W. Choi, S. Choi, T. H. Yoo, H.-J. An, S. C. An, J. Lee, J. Choi, S.-Y. Kim, J.-S. Lee, S. Lee, J. Choi and J. M. Kim, *Adv. Sci.*, 2025, **12**, 2415626.
- 23 M. Gazorpak, K. M. Hugentobler, D. Paul, P.-L. Germain, M. Kretschmer, I. Ivanova, S. Frei, K. Mathis, R. Rudolf, S. Mompert Barrenechea, V. Fischer, X. Xue, A. L. Ptaszek, J. Holzinger, M. Privitera, A. Hierlemann, O. C. Meijer, R. Konrat, E. M. Carreira, J. Bohacek and K. Gapp, *Nat. Commun.*, 2023, **14**, 8177.
- 24 J. a. Ji, Y. Jin, S. Ma, Y. Zhu, X. Bi, Q. You and Z. Jiang, *J. Med. Chem.*, 2024, **67**, 12521.
- 25 C. Zhou, C. Sun, M. Huang, X. Tang, L. Pi and C. Li, *J. Med. Chem.*, 2024, **67**, 15168.
- 26 Y.-L. Tseng, P.-C. Lu, C.-C. Lee, R.-Y. He, Y.-A. Huang, Y.-C. Tseng, T.-J. R. Cheng, J. J.-T. Huang and J.-M. Fang, *J. Biomed. Sci.*, 2023, **30**, 27.
- 27 N. Zhao, J. S. Y. Ho, F. Meng, S. Zheng, A. P. Kurland, L. Tian, M. Rea-Moreno, X. Song, J.-S. Seo, H. Ü. Kaniskan, A. J. W. te Velthuis, D. Tortorella, Y.-W. Chen, J. R. Johnson, J. Jin and I. Marazzi, *Cell Host Microbe*, 2023, **31**, 1154.
- 28 P. Gunasekaran, Y. S. Hwang, G.-H. Lee, J. Park, J. G. Kim, Y. K. La, N. Y. Park, R. Kothandaraman, M. S. Yim, J. Choi, H. N. Kim, I. Y. Park, S. J. Lee, M.-H. Kim, H. Cha-Molstad, S. Y. Shin, E. K. Ryu and J. K. Bang, *J. Med. Chem.*, 2024, **67**, 3307.
- 29 Z. Zhou, G. Zhou, C. Zhou, Z. Fan, R. Cui, Y. Li, R. Li, Y. Gu, H. Li, Z. Ge, X. Cai, B. Jiang, D. Wang, M. Zheng, T. Xu and S. Zhang, *J. Med. Chem.*, 2023, **66**, 4197.
- 30 A. Kaneshige, Y. Yang, L. Bai, M. Wang, R. Xu, L. Mallik, K. Chinnaswamy, H. Metwally, Y. Wang, D. McEachern, J. Tošović, C.-Y. Yang, P. D. Kirchhoff, J. L. Meagher, J. A. Stuckey and S. Wang, *J. Med. Chem.*, 2025, **68**, 5125.
- 31 Y. Chen, W. Li, S. Kwon, Y. Wang, Z. Li and Q. Hu, *J. Am. Chem. Soc.*, 2023, **145**, 9815.
- 32 G. Wilms, K. Schofield, S. Maddern, C. Foley, Y. Shaw, B. Smith, L. E. Basantes, K. Schwandt, A. Babendreyer, T. Chavez, N. McKee, V. Gokhale, S. Kallabis, F. Meissner, S. N. Rokey, T. Dunckley, W. R. Montfort, W. Becker and C. Hulme, *J. Med. Chem.*, 2024, **67**, 17259.
- 33 T. Wu, Z. Zhang, G. Gong, Z. Du, Y. Xu, S. Yu, F. Ma, X. Zhang, Y. Wang, H. Chen, S. Wu, X. Xu, Z. Qiu, Z. Li, H. Wu, J. Bian and J. Wang, *Eur. J. Med. Chem.*, 2023, **260**, 115774.
- 34 B. Zhang, C. Liu, Z. Yang, S. Zhang, X. Hu, B. Li, M. Mao, X. Wang, Z. Li, S. Ma, S. Zhang and C. Qin, *J. Med. Chem.*, 2023, **66**, 11158.
- 35 S. Chen, Z. Chen, L. Lu, Y. Zhao, R. Zhou, Q. Xie, Y. Shu, J. Lin, X. Yu and Y. Wang, *Eur. J. Med. Chem.*, 2023, **255**, 115403.
- 36 J. A. Jarusiewicz, S. Yoshimura, M. Actis, Y. Li, X. Fu, L. Yang, S. Narina, S. M. Pruett-Miller, S. Zhou, X. Wang, A. A. High, G. Nishiguchi, J. J. Yang and Z. Rankovic, *J. Med. Chem.*, 2024, **67**, 11868.
- 37 Y. He, Y. Zheng, C. Zhu, P. Lei, J. Yu, C. Tang, H. Chen and X. Diaoy, *J. Med. Chem.*, 2024, **67**, 14277.
- 38 S. Ying, H. Chi, X. Wu, P. Zeng, J. Chen, T. Fu, W. Fu, P. Zhang and W. Tan, *J. Med. Chem.*, 2024, **67**, 17053.
- 39 L. Zhou, K. Zhou, Y. Chang, J. Yang, B. Fan, Y. Su, Z. Li, R. Mannan, S. Mahapatra, M. Ding, F. Zhou, W. Huang, X. Ren, J. Xu, G. X. Wang, J. Zhang, Z. Wang, A. M. Chinnaiyan and K. Ding, *J. Med. Chem.*, 2024, **67**, 18247.
- 40 J. X. Qiao, D. Williams, P. Gill, L. Li, D. Norris, J. S. Tokarski, J. Wong, H. Qi, Y. Hafeji, D. P. Downes, B. Degnen, Y.-K. Wang, G. Locke, H. Fang, F. Yu, S. Xu, J. Naglich, J. Zhang, P. Nanjappa, C. Dai, L. Chourb, J. Napoline, R. Tester, C. Jorge, Y.-X. Li, A. Mathur, C. Barbieri,



- M. G. Soars, A. Venkatanarayan, E. Lees, R. M. Borzilleri, A. V. Gavai, M. Wichroski and T. G. M. Dhar, *J. Med. Chem.*, 2024, **67**, 19736.
- 41 L. Yang, W. Tu, L. Huang, B. Miao, A. Kaneshige, W. Jiang, L. Leng, M. Wang, B. Wen, D. Sun and S. Wang, *J. Med. Chem.*, 2023, **66**, 10761.
- 42 Z. Chen, B. Hu, R. K. Rej, D. Wu, R. K. Acharyya, M. Wang, T. Xu, J. Lu, H. Metwally, Y. Wang, D. McEachern, L. Bai, C. L. Gersch, M. Wang, W. Zhang, Q. Li, B. Wen, D. Sun, J. M. Rae and S. Wang, *J. Med. Chem.*, 2023, **66**, 12559.
- 43 R. K. Rej, B. Hu, Z. Chen, R. K. Acharyya, D. Wu, H. Metwally, D. McEachern, Y. Wang, W. Jiang, L. Bai, L. S. Nishimura, C. L. Gersch, M. Wang, B. Wen, D. Sun, K. Carlson, J. A. Katzenellenbogen, G. Xu, W. Zhang, W. Wu, E. S. Priestley, Z. Sui, J. M. Rae and S. Wang, *J. Med. Chem.*, 2024, **67**, 20933.
- 44 C. Wang, M. Wang, Y. Wang, R. K. Rej, A. Aguilar, T. Xu, L. Bai, J. Tošović, D. McEachern, Q. Li, F. Sarkari, B. Wen, D. Sun and S. Wang, *J. Med. Chem.*, 2024, **67**, 14125.
- 45 R. K. Acharyya, R. K. Rej, B. Hu, Z. Chen, D. Wu, J. Lu, H. Metwally, D. McEachern, Y. Wang, W. Jiang, L. Bai, J. Tošović, C. L. Gersch, G. Xu, W. Zhang, W. Wu, E. S. Priestley, Z. Sui, F. Sarkari, B. Wen, D. Sun, J. M. Rae and S. Wang, *J. Med. Chem.*, 2024, **67**, 19010.
- 46 J. Dong, J. Miao, Y. Miao, Z. Qu, S. Zhang, P. Zhu, F. Wiede, B. A. Jassim, Y. Bai, Q. Nguyen, J. Lin, L. Chen, T. Tiganis, W. A. Tao and Z.-Y. Zhang, *Angew. Chem., Int. Ed.*, 2023, **62**, e202303818.
- 47 M. Schiedel, D. Herp, S. Hammelmann, S. Swyter, A. Lehotzky, D. Robaa, J. Oláh, J. Ovádi, W. Sippl and M. Jung, *J. Med. Chem.*, 2018, **61**, 482.
- 48 A. Zagidullin, V. Milyukov, A. Rizvanov and E. Bulatov, *Explor. Targeted Anti-Tumor Ther.*, 2020, **1**, 381.
- 49 G. Q. Weng, C. Shen, D. S. Cao, J. B. Gao, X. W. Dong, Q. J. He, B. Yang, D. Li, J. Wu and T. J. Hou, *Nucleic Acids Res.*, 2021, **49**, D1381.
- 50 G. Q. Weng, X. Y. Cai, D. S. Cao, H. Y. Du, C. Shen, Y. F. Deng, Q. J. He, B. Yang, D. Li and T. J. Hou, *Nucleic Acids Res.*, 2023, **51**, D1367.
- 51 J. X. Ge, S. M. Li, G. Q. Weng, H. T. Wang, M. J. Fang, H. Y. Sun, Y. F. Deng, C. Y. Hsieh, D. Li and T. J. Hou, *Nucleic Acids Res.*, 2024, **53**, D1510.
- 52 S. Imaide, K. M. Riching, N. Makukhin, V. Vetma, C. Whitworth, S. J. Hughes, N. Trainor, S. D. Mahan, N. Murphy, A. D. Cowan, K.-H. Chan, C. Craigon, A. Testa, C. Maniaci, M. Urh, D. L. Daniels and A. Ciulli, *Nat. Chem. Biol.*, 2021, **17**, 1157.
- 53 M. Zheng, J. Huo, X. Gu, Y. Wang, C. Wu, Q. Zhang, W. Wang, Y. Liu, Y. Liu, X. Zhou, L. Chen, Y. Zhou and H. Li, *J. Med. Chem.*, 2021, **64**, 7839.
- 54 M. Scaranti, E. Cojocar, S. Banerjee and U. Banerji, *Nat. Rev. Clin. Oncol.*, 2020, **17**, 349.
- 55 J. Liu, H. Chen, Y. Liu, Y. Shen, F. Meng, H. Ü. Kaniskan, J. Jin and W. Wei, *J. Am. Chem. Soc.*, 2021, **143**, 7380.
- 56 A. G. Bond, M. Muñoz i Ordoño, C. M. Bisbach, C. Craigon, N. Makukhin, E. A. Caine, M. Nagala, M. Urh, G. E. Winter, K. M. Riching and A. Ciulli, *J. Am. Chem. Soc.*, 2024, **146**, 33675.
- 57 S. M. Kondengadan, S. Bansal, C. Yang, D. Liu, Z. Fultz and B. Wang, *Acta Pharm. Sin. B*, 2023, **13**, 1990.
- 58 Q. Zhang, G. Kuang, L. Wang, P. Duan, W. Sun and F. Ye, *Research*, 2023, **6**, 0251.
- 59 H. Lebraud, D. J. Wright, C. N. Johnson and T. D. Heightman, *ACS Cent. Sci.*, 2016, **2**, 927.
- 60 X. Teng, X. Zhao, Y. Dai, X. Zhang, Q. Zhang, Y. Wu, D. Hu and J. Li, *J. Am. Chem. Soc.*, 2024, **146**, 27382.
- 61 S. Xie, J. Zhu, Y. Peng, F. Zhan, F. Zhan, C. He, D. Feng, J. Xie, J. Liu, H. Zhu, H. Yao, J. Xu, Z. Su and S. Xu, *Angew. Chem., Int. Ed.*, 2025, **64**, e202421713.
- 62 D. Thang Cong, J. W. Lau, C. Sun, S. Liu, K. T. Kha, S. T. Lim, Y. Y. Oon, Y. P. Kwan, J. J. Ma, Y. Mu, X. Liu, T. J. Carney, X. Wang and B. Xing, *Sci. Adv.*, 2022, **8**, eabq2216.
- 63 S. Sahu, A. S. Amrutha and N. Tamaoki, *Med. Res. Rev.*, 2025, **45**, 1142.
- 64 P. Pfaff, K. T. G. Samarasinghe, C. M. Crews and E. M. Carreira, *ACS Cent. Sci.*, 2019, **5**, 1682.
- 65 Y.-H. Jin, M.-C. Lu, Y. Wang, W.-X. Shan, X.-Y. Wang, Q.-D. You and Z.-Y. Jiang, *J. Med. Chem.*, 2020, **63**, 4644.
- 66 M. Reynders, B. S. Matsuura, M. Bérouti, D. Simoneschi, A. Marzio, M. Pagano and D. Trauner, *Sci. Adv.*, 2020, **6**, eaay5064.
- 67 T. Ko, C. Jou, A. B. Grau-Perales, M. Reynders, A. A. Fenton and D. Trauner, *ACS Chem. Neurosci.*, 2023, **14**, 3704.
- 68 Q. Zhang, C. S. Kounde, M. Mondal, J. L. Greenfield, J. R. Baker, S. Kotelnikov, M. Ignatov, C. P. Tinworth, L. Zhang, D. Conole, E. De Vita, D. Kozakov, A. McCluskey, J. D. Harling, M. J. Fuchter and E. W. Tate, *Chem. Commun.*, 2022, **58**, 10933.
- 69 J. Cheng, J. Zhang, S. He, M. Li, G. Dong and C. Sheng, *Angew. Chem., Int. Ed.*, 2024, **63**, e202315997.
- 70 J. Zhang, L. K. Herzog, D. P. Corkery, T.-C. Lin, L. Klewer, X. Chen, X. Xin, Y. Li and Y.-W. Wu, *Angew. Chem., Int. Ed.*, 2025, **64**, e202416456.
- 71 M. Ouyang, Y. Feng, H. Chen, Y. Liu, C. Tan and Y. Tan, *Bioengineering*, 2023, **10**, 1368.
- 72 G. Xue, K. Wang, D. Zhou, H. Zhong and Z. Pan, *J. Am. Chem. Soc.*, 2019, **141**, 18370.
- 73 Y. Chen, S. Pal, W. Li, F. Liu, S. Yuan and Q. Hu, *Nat. Biotechnol.*, 2024, DOI: [10.1038/s41587-024-02494-8](https://doi.org/10.1038/s41587-024-02494-8).
- 74 J. Zhong, R. Zhao, Y. Wang, Y.-x. Su and X. Lan, *Nanoscale*, 2024, **16**, 4378.
- 75 F. Yang, Q. Luo, Y. Wang, H. Liang, Y. Wang, Z. Hou, C. Wan, Y. Wang, Z. Liu, Y. Ye, L. Zhu, J. Wu, F. Yin and Z. Li, *J. Am. Chem. Soc.*, 2023, **145**, 7879.
- 76 C. Song, Z. Jiao, Z. Hou, R. Wang, C. Lian, Y. Xing, Q. Luo, Y. An, F. Yang, Y. Wang, X. Sha, Z. Ruan, Y. Ye, Z. Liu, Z. Li and F. Yin, *J. Am. Chem. Soc.*, 2023, **145**, 21860.
- 77 C. Song, Z. Jiao, Z. Hou, Y. Xing, X. Sha, Y. Wang, J. Chen, S. Liu, Z. Li and F. Yin, *JACS Au*, 2024, **4**, 2915.
- 78 N.-Y. Zhang, D.-Y. Hou, X.-J. Hu, J.-X. Liang, M.-D. Wang, Z.-Z. Song, L. Yi, Z.-J. Wang, H.-W. An, W. Xu and H. Wang, *Angew. Chem., Int. Ed.*, 2023, **62**, e202308049.



- 79 C. Zhang, S. He, Z. Zeng, P. Cheng and K. Pu, *Angew. Chem., Int. Ed.*, 2022, **61**, e202114957.
- 80 J. Sun, M. Gu, L. Peng, J. Guo, P. Chen, Y. Wen, F. Feng, X. Chen, T. Liu, Y. Chen, X. Lu, L. Gao, S. Q. Yao and P. Yuan, *J. Am. Chem. Soc.*, 2025, **147**, 372.
- 81 Y. Wang, L. Han, F. Liu, F. Yang, X. Jiang, H. Sun, F. Feng, J. Xue and W. Liu, *Colloids Surf., B*, 2020, **188**, 110795.
- 82 Y. Ding, D. Xing, Y. Fei and B. Lu, *Chem. Soc. Rev.*, 2022, **51**, 8832.
- 83 Y.-y. Li, Y. Yang, R.-s. Zhang, R.-x. Ge and S.-b. Xie, *Acta Pharmacol. Sin.*, 2025, **46**, 1.
- 84 J. Zhang, X. Pan, W. Ji and J. Zhou, *Bioorg. Chem.*, 2024, **149**, 107466.
- 85 M. Xu, Y. Hu, J. Wu, J. Liu and K. Pu, *J. Am. Chem. Soc.*, 2024, **146**, 34669.
- 86 M. Ye, J. Hu, M. Peng, J. Liu, J. Liu, H. Liu, X. Zhao and W. Tan, *Int. J. Mol. Sci.*, 2012, **13**, 3341.
- 87 Y. Wu, B. Lin, Y. Lu, L. Li, K. Deng, S. Zhang, H. Zhang, C. Yang and Z. Zhu, *Angew. Chem., Int. Ed.*, 2023, **62**, e202218106.
- 88 W. Sun, H. Zhang, W. Xie, L. Ma, Y. Dang, Y. Liu, L. Li, F. Qu and W. Tan, *J. Am. Chem. Soc.*, 2024, **146**, 25490.
- 89 Q. Duan, H.-R. Jia, W. Chen, C. Qin, K. Zhang, F. Jia, T. Fu, Y. Wei, M. Fan, Q. Wu and W. Tan, *Adv. Sci.*, 2024, **11**, 2308924.
- 90 L. Zhao, J. Zhao, K. Zhong, A. Tong and D. Jia, *Signal Transduct. Target. Ther.*, 2022, **7**, 113.
- 91 L. Mei, X. Chen, F. Wei, X. Huang, L. Liu, J. Yao, J. Chen, X. Luo, Z. Wang and A. Yang, *Autophagy*, 2023, **19**, 2997.
- 92 J. Pei, X. Pan, A. Wang, W. Shuai, F. Bu, P. Tang, S. Zhang, Y. Zhang, G. Wang and L. Ouyang, *Chem. Commun.*, 2021, **57**, 13194.
- 93 D. Takahashi, T. Ora, S. Sasaki, N. Ishii, T. Tanaka, T. Matsuda, M. Ikeda, J. Moriyama, N. Cho, H. Nara, H. Maezaki, M. Kamaura, K. Shimokawa and H. Arimoto, *J. Med. Chem.*, 2023, **66**, 12342.
- 94 G. Dong, Y. Wu, J. Cheng, L. Chen, R. Liu, Y. Ding, S. Wu, J. Ma and C. Sheng, *J. Med. Chem.*, 2022, **65**, 7619.
- 95 J. Bao, Z. Chen, Y. Li, L. Chen, W. Wang, C. Sheng and G. Dong, *ACS Med. Chem. Lett.*, 2024, **15**, 29.
- 96 Z. Ouyang, M. Ma, Z. Zhang, H. Wu, Y. Xue, Y. Jian, K. Yin, S. Yu, C. Zhao, W. Guo and X. Gu, *J. Med. Chem.*, 2024, **67**, 433.
- 97 Z. Zhu, J. Li, S. Shen, H. Al-furas, S. Li, Y. Tong, Y. Li, Y. Zeng, Q. Feng, K. Chen, N. Ma, F. Zhou, Z. Zhang, Z. Li, J. Pang, K. Ding and F. Xu, *Eur. J. Med. Chem.*, 2024, **270**, 116345.
- 98 D. A. Nalawansa, K. Mangano, W. den Besten and P. R. Potts, *ChemBioChem*, 2024, **25**, e202300712.
- 99 S. Tan, Z. Chen, R. Lu, H. Liu and X. Yao, *Wires. Comput. Mol. Sci.*, 2025, **15**, e70013.
- 100 M. Scheepstra, K. F. W. Hekking, L. van Hijfte and R. H. A. Folmer, *Comput. Struct. Biotech.*, 2019, **17**, 160.
- 101 D. Pliatsika, C. Blatter and R. Riedl, *Drug Discov. Today*, 2024, **29**, 104178.
- 102 C. Wang, Y. Zhang, W. Chen, Y. Wu and D. Xing, *Mol. Cancer*, 2024, **23**, 110.

